

Marquette University

e-Publications@Marquette

***Electrical and Computer Engineering Faculty Research and Publications/College of Engineering***

***This paper is NOT THE PUBLISHED VERSION; but the author's final, peer-reviewed manuscript.*** The published version may be accessed by following the link in the citation below.

*Proceedings of SPIE 8973: Micromachining and Microfabrication Process Technology XIX*, No. 8973 (March 2014). [DOI](#). This article is © Society of Photo-optical Instrumentation Engineers (SPIE) and permission has been granted for this version to appear in [e-Publications@Marquette](#). Society of Photo-optical Instrumentation Engineers (SPIE) does not grant permission for this article to be further copied/distributed or hosted elsewhere without the express permission from Society of Photo-optical Instrumentation Engineers (SPIE).

# Fabrication of Microelectromechanical Systems (MEMS) Cantilevers for Photoacoustic (PA) Detection of Terahertz (THz) Radiation

R. Newberry

Air Force Institute of Technology

N. Glauvitz

Air Force Institute of Technology

R.A. Coutu

Air Force Institute of Technology

I.R. Medvedev

Wright State University

D. Petkie

Wright State University

## Abstract

Historically, spectroscopy has been a cumbersome endeavor due to the relatively large sizes (3ft – 100ft in length) of modern spectroscopy systems. Taking advantage of the photoacoustic effect would allow for much smaller absorption chambers since the photoacoustic (PA) effect is independent of the absorption path length. In order to detect the photoacoustic waves being generated, a photoacoustic microphone would be required. This paper reports on the fabrication efforts taken in order to create microelectromechanical systems (MEMS) cantilevers for the purpose of sensing photoacoustic waves generated via terahertz (THz) radiation passing through a gaseous sample. The cantilevers are first modeled through the use of the finite element modeling software, CoventorWare<sup>®</sup>. The cantilevers fabricated with bulk micromachining processes and are 7x2x0.010mm on a silicon-on-insulator (SOI) wafer which acts as the physical structure of the cantilever. The devices are released by etching through the wafer's backside and etching through the buried oxide with hydrofluoric acid. The cantilevers are placed in a test chamber and their vibration and deflection are measured via a Michelson type interferometer that reflects a laser off a gold tip evaporated onto the tip of the cantilever. The test chamber is machined from stainless steel and housed in a THz testing environment at Wright State University. Fabricated devices have decreased residual stress and larger radii of curvatures by approximately 10X.

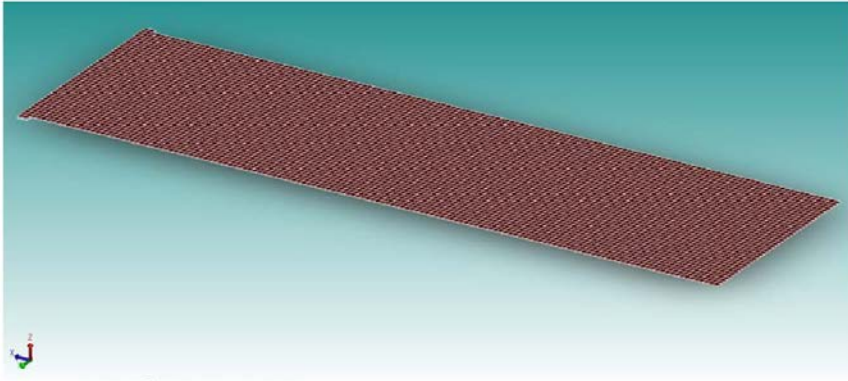
## 1. INTRODUCTION

Many techniques have been employed over the last several decades for photoacoustic chemical sensing of trace gases and molecular analysis. Photoacoustic detection of radiation is an experimental technique widely used for molecular spectral detection in solids and gasses.<sup>1,3</sup> In this research, a microelectromechanical systems (MEMS) cantilever was designed, modeled, and fabricated in order to create an optically measured, photoacoustic sensor responsive to a spectrum of sub-millimeter/terahertz radiation. The photoacoustic effect results when energy from an electromagnetic wave is absorbed by molecules and collisionally transferred through nonradiative pathways into translational energy.<sup>4</sup> If the radiation produced by the source is properly modulated and enough of the energy is absorbed by a gaseous species, an acoustic wave results which can be detected by a pressure sensitive device.<sup>5</sup> The novelty of this effort is the combination of three factors; acoustic cell size, the radiation source, and the ability to collect displacement data from a MEMS cantilever with a Michelson type interferometer. A finite element model of the cantilever is presented, followed by the fabrication process.

## 2. MODELING

Initial analytical design calculations similar to ones developed in<sup>2</sup> showed that a silicon cantilever 5x2x0.010 mm<sup>3</sup> (length x width x thickness) should produce the needed deflection to generate an adequate measurement from a Michelson-type interferometer. Finite Element modeling of the cantilever displacement over a range of applied pressures was performed in CoventorWare<sup>®</sup> finite element software. Shown in **Figure 1** is a model of a cantilever designed with the dimensions listed above and showed a tip deflection of 0.21  $\mu\text{m}$  for a 0.1 mPa applied load. Fine tuning of the model will be accomplished using interferometric data obtained in the acoustic test chamber.

**Figure 1:** CoventorWare® finite element simulation of a 7x2x0.01mm cantilever photoacoustic sensor with simulation mesh parameter of 50x50µm, extruded 10µm in the z-direction



Cantilever bending in an underdamped system can be expressed through analytical models where the tip displacement  $A$  is given by

$$A(\omega) = \frac{F}{m\sqrt{(\omega_0^2 - \omega^2)^2 + 4\left(\frac{1}{\tau}\right)^2\omega^2}} \cong \frac{F\tau}{2m\omega} \quad (1)$$

Where  $\tau$  is the time constant,  $m$  is the mass of the cantilever,  $F$  is the applied force,  $\omega$  is angular frequency, and  $\omega_0$  the angular resonant frequency.<sup>3</sup> An examination of this equation reveals that an increase in time constant, reduction in mass, and reduction in resonant frequency will allow for larger deflections for a given force. A cantilever's resonant frequency  $f_0$  is described by

$$f_0 = \frac{1}{2\pi} \sqrt{\frac{k}{m_{eff}}} \quad (2)$$

Where  $k$  is the spring constant and  $m_{eff}$  is the effective mass of the cantilever.<sup>3</sup> The spring constant of a cantilever beam can be described by

$$k = \frac{2}{3} E_y w \left(\frac{h}{L}\right)^3 \quad (3)$$

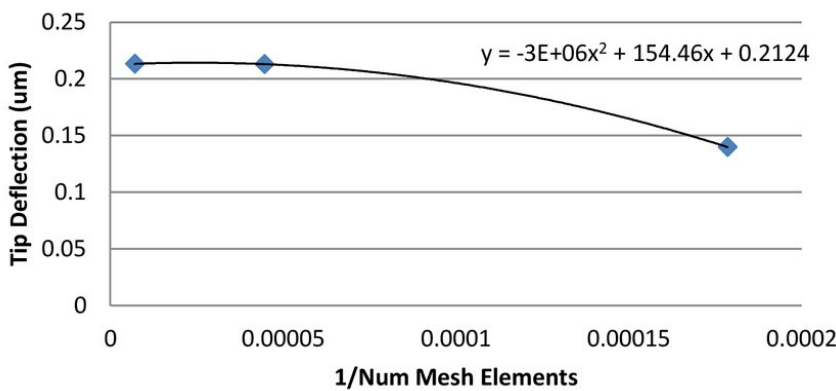
Where  $E_y$  is the Young's modulus of the material and the other parameters are cantilever dimensions of length ( $L$ ), width ( $w$ ), and thickness ( $h$ ). An analysis of these equations yields that in general, thinner, longer, narrower cantilevers will yield optimal tip deflection, but careful consideration must be taken into fragility of devices. Larger length to thickness ratios will lead to difficult to fabricate devices.

Initial cantilever designs were evaluated through the use of CoventorWare Finite Element Modeling (FEM) Software. Using a harmonic modal analysis tool, a harmonic pressure load was applied to the cantilever surface as a function of frequency and the magnitude of the tip displacement was recorded. A limitation of the modeling software is the finite elements. **Figure 1** shows a simulated cantilever with a 50x50µm mesh extruded 10µm in the z-direction.

A 50x50µm mesh is the largest mesh size used in modeling this cantilever, but still results in 5,600 mesh elements across the entire length of the beam. Each mesh element must be simulated for during the entire frequency spectrum and through the modal harmonics, which results in a large number of computations. The finest mesh of 10x10x10µm blocks yields in 140,000 mesh elements.

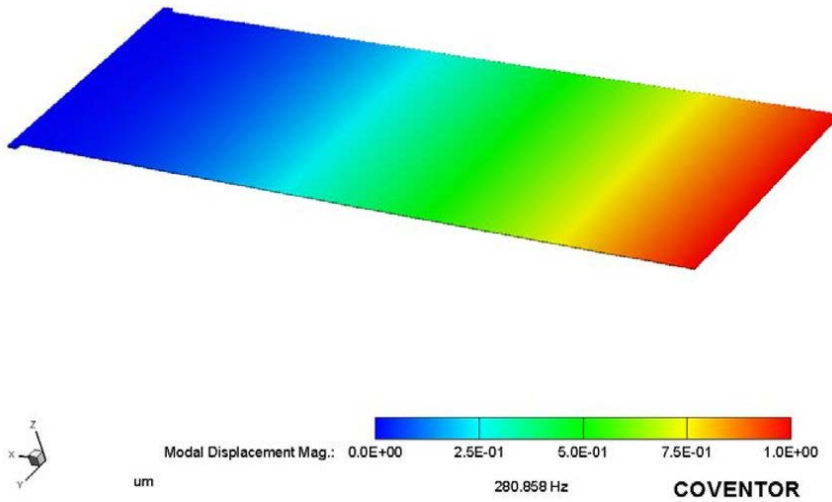
To increase the number of elements allows for more accurate simulations, but is very computationally demanding. This increase in computing time is nonconductive to running many simulations and a diminishing returns effect can be seen. As such, a mesh analysis was performed to find a suitable minimum elemental mesh size to obtain accurate results. shows a mesh analysis performed on CoventorWare for a simulated 7x2x0.01mm cantilever.

**Figure 2:** Mesh Analysis performed with Finite Element Modeling (FEM) software, CoventorWare® on a 7x2x0.01mm cantilever under a 0.1mPa load. This study shows that as the number of mesh elements approaches infinity, the simulations approach a cantilever deflection of 0.2124µm which is used as a true value.



This mesh analysis shows a cantilever beam under a 0.1mPA pressure load applied along the surface. This mesh study indicates that as the number of mesh elements approaches infinity, in other words, 1/number of mesh elements approaches 0, the tip deflection should approach a value of 0.214µm. This study is important in justifying larger meshes, which significantly reduces computation times. An increase in mesh size from 10µm to 25µm reduces run times by over 50% but only yields in a difference in results of 0.26% and an error from the estimated “true value” of 0.48%. With a suitable sized mesh, a proper series of simulations may be run to simulated cantilever bending, resonant frequency, modal harmonics, and various other cantilever aspects. shows a completed CoventorWare simulation with the first modal harmonic being displayed.

**Figure 3:** CoventorWare® finite element model of cantilever deflection for a static 0.1mPa applied load with a modal harmonic at 280.8Hz



This simulation shows the first modal harmonic of the cantilever appearing at 280.858 Hz and shows the modal displacement magnitude along the surface of the beam at a 0.1mPa pressure load.

### 3. FABRICATION

Based on the modelled results, a cantilever design was designed and fabricated using MEMS fabrication processes. The fabrication process is done on an n-type silicon-on-insulator (SOI) wafer. All fabrication is done on-site in the clean rooms of either the Air Force Institute of Technology (AFIT) or the Air Force Research Laboratory (AFRL). First, a thin layer (200/1000 Å) of titanium/Gold (Ti/Au) is evaporated onto the tip of the cantilever as a reflective surface for the interferometer. The titanium acts as an adhesion layer for the gold, which does not normally stick very well to silicon. Next, the device layer is patterned, with photoresist and exposed in an MJB3 mask aligner with the proper device layer mask. It is exposed with UV light for 8.2s and receives a power dosage of approximately 150mJ/cm<sup>2</sup> in order to pattern the resist which is then developed and baked. Next, the sample is etched via DRIE to gap the device layer from the surrounding membrane as shown in **Figure 4 (A)**. This gap distance must be tightly controlled for if it is too large, it allows for gas leakage between the cantilever and surrounding membrane.

**Figure 4:** Cantilever fabrication process steps, (A) begin with initial substrate, (B) etch device layer via deep reactive ion etching (DRIE) to form cantilever shape from substrate, (C) DRIE backside of handle wafer to the buried oxide, leaving only oxide as structural support, and (D) remove buried oxide below cantilever to fully release cantilever.

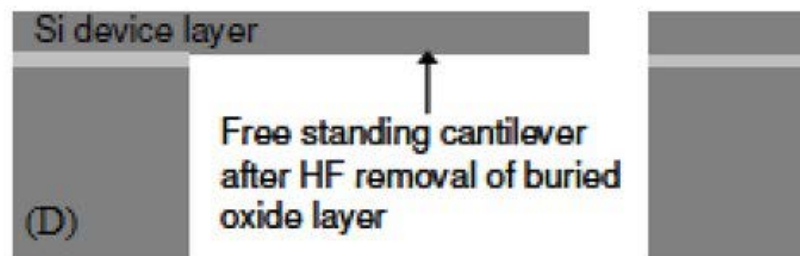
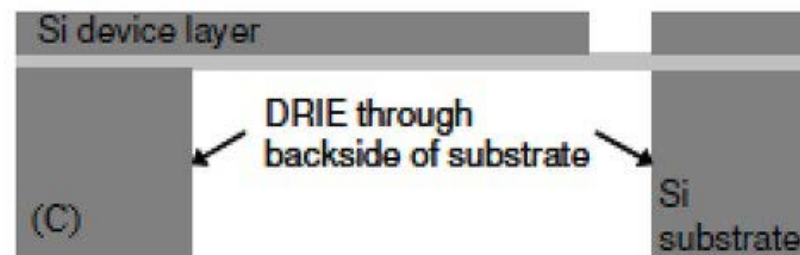
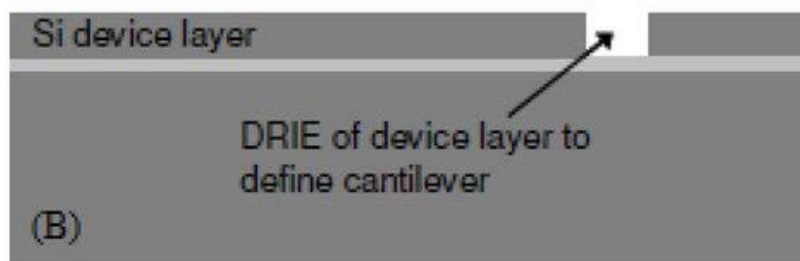
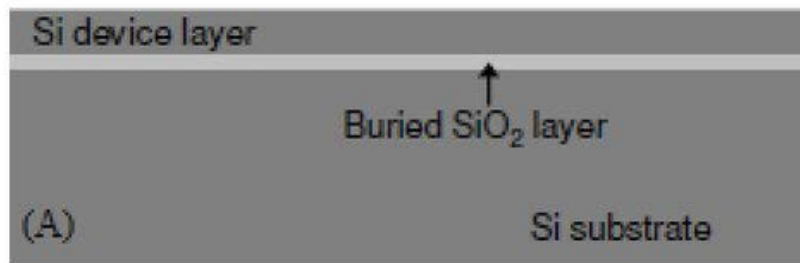
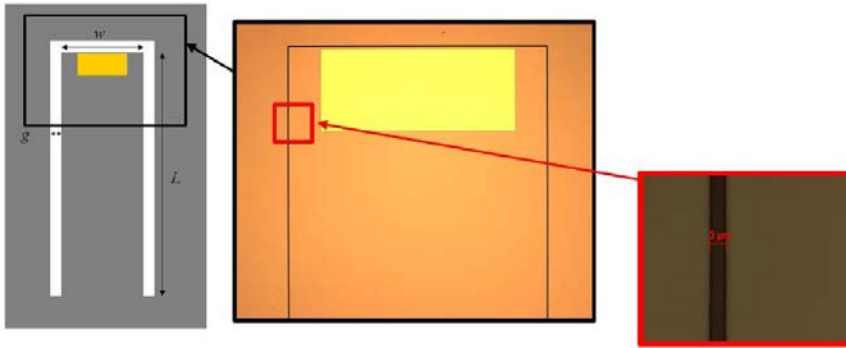


**Figure 5:** Schematic of the gap between the cantilever and the surrounding membrane along with an optical image of the cantilever. A close-up of the image shows a  $3\mu\text{m}$  gap on this cantilever.



#### 4. EXPERIMENTAL TEST SETUP

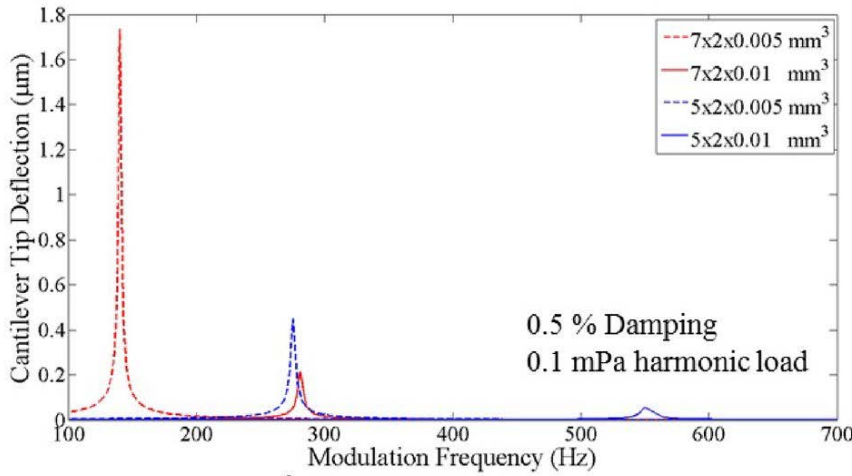
The photoacoustic test chamber is designed to allow for both piezoelectric voltage signal and laser interferometer data measurements from cantilever deflection. Since the sensing element for the acoustic chamber is a MEMS cantilever; two types of cantilevers were initially planned for fabrication in the device layer of a SOI wafer. The samples here are made consisted of a bare silicone cantilever and later piezoelectric devices are planned on being made. Initially tests using a Michelson type laser interferometer were used to measure the deflection of a plain silicon cantilever. Preliminary results from the laser interferometer are promising but not yet complete. Data collection is triggered by the signal generator; electrical signals from the cantilever transducer and the laser interferometer will be synchronized.

The cylindrical acoustic absorption cell cavity is 2 inches long and has a 5 mm radius. Pressure in the chamber can be controlled over a wide range from low mtorr all the way up to atmospheric pressure. An advantage of this experimental setup is that the radiation source is capable of producing precise frequencies over a broad spectral range. Radiation source frequencies from 0.1-1 THz can be achieved. Radiation source modulation frequencies can be amplitude modulated on/off with a standard 50/50 duty cycle or operated in a duty cycle controlled mode where both the on and off durations can be specified. The duty cycle controlled mode is advantageous for testing these devices over different pressure ranges since the cantilever damping and deflection change with pressure.

#### 5. RESULTS

This fabrication process improves upon prior research done at AFIT by increasing the length of the cantilever from the previous 5mm to the current 7mm. **Figure 6** shows simulation results and the predicted improvements that can be achieved by increasing a cantilever length by 2mm.

**Figure 6:** Simulation results from CoventorWare® that shows the deflections for varying dimensions of cantilever under the same 0.1mPa harmonic load with 0.5% damping coefficient. In general, the longer and thinner a cantilever becomes, the more it deflects.



According to **Figure 6**, by lengthening the cantilever, a 10µm thick device will experience up to 4 times more deflection under the same pressure loads and a 0.5% damping coefficient. The damping coefficient is the percentage of the critical damping coefficient, and 0.5% simulates a low pressure environment. For now, this research only involves a 10µm thick cantilever beam, as 5µm devices are fragile and difficult to fabricate.

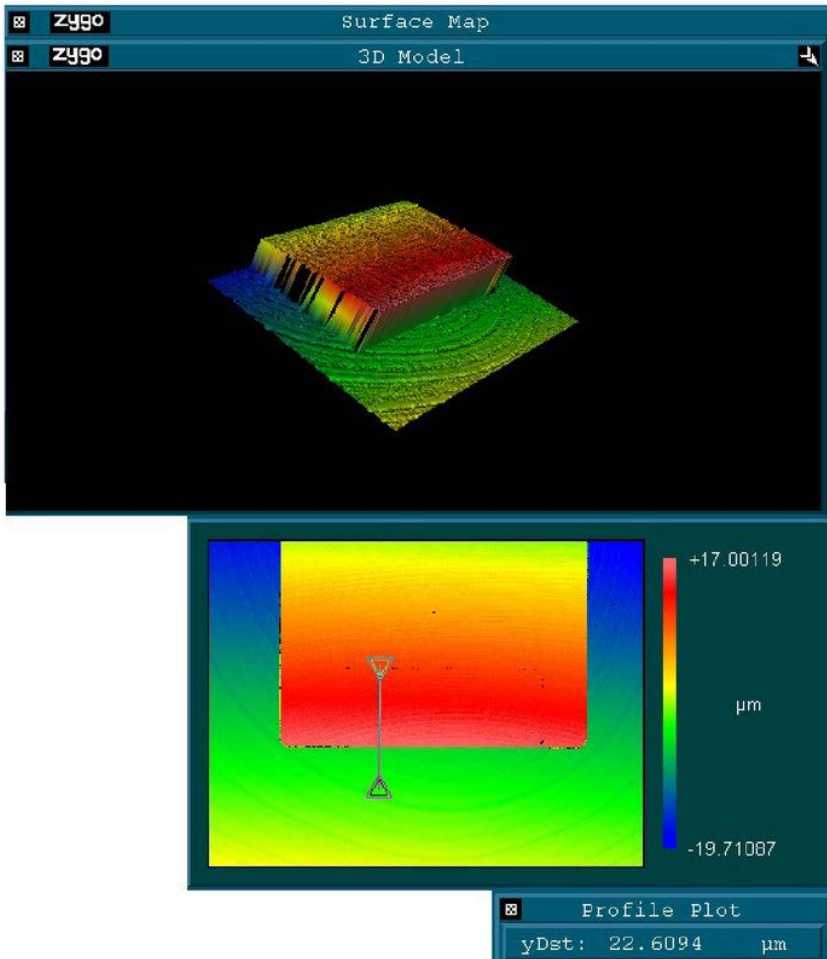
Also, the membranes surrounding the cantilever tend to snap and develop hairline fractures due to the high stress concentration that builds up around the corner of the membrane, surrounding the cantilever tip.<sup>6</sup> This high stress concentration along with a very long length to thickness ratio (700) makes the cantilever very fragile and difficult to fabricate and handle once released.

Another limitation of the sensitivity of the cantilever is the resting curvature of the devices. The internal stress gradient along the surface of the beam causes the cantilever to rest out of plane, which limits deflection and damping, due to gas leakage. **Figure 7** shows this deflection out of plane being measured with the use of a Zygo® white-light interferometer. At rest, the cantilever has a radius of curvature of 1.1m. Using this, and Stoley’s equation:

$$\frac{1}{R} = \frac{6(1-\nu)\Delta\sigma}{E_{\gamma}d^2} \tag{4}$$



**Figure 7:** 3D surface model and profile plot of resting cantilever using a Zygo® white-light interferometer. The image shows how, at rest, the tip of a 7x2x0.01mm cantilever is 22µm above the surrounding membrane. This gap is a source of gas leakage and sensitivity loss.



Where  $R = 1.11$  m is the radius of curvature,  $E_y = 169$  GPa is the Young’s Modulus for silicon,  $\nu = 0.064$  is Poisson’s ratio corresponding to the crystal orientation of the bending cantilever, and  $d = 10$  µm is the thickness of our beam. It is calculated that residual stress in a fabricated and released cantilever beam  $\Delta\sigma = 2.702$  N/m.

This radius of curvature is improved from earlier 10µm devices fabricated at AFIT, that had a radius of curvature of 0.114 m, resulting in residual stress of 26.40 N/m. Refinements in fabrication processes and the increased length of the cantilevers leads to nearly a 10X improvement in radius of curvature and residual stress along the length of the beam.

## 6. CONCLUSIONS

In this effort a MEMS cantilever sensor was designed, modeled, fabricated, and preliminary photoacoustic data was collected with the laser interferometer configuration. The next phase will be to fabricate and test a 7x2x0.05mm cantilever in the chamber and refine the mechanical design. The result of this research is photoacoustic detection that is independent of the absorption path length. This is a great advantage in comparison to traditional methods of detecting radiation and may lead to hand held THz chemical sensors and detector arrays for imaging.

## Acknowledgements

The authors would like to thank the Air Force Research Laboratory (AFRL) Sensors and Propulsion Directorates for their assistance, use of their resources, and facilities. The authors also thank the technical support and dedicated work of AFIT's own cleanroom staff, Rich Johnston and Thomas Stephenson.

**Disclaimer:** The views expressed in this article are those of the authors and do not reflect the official policy or position of the United States Air Force, Department of Defense, or the United States Government.

## References

- [1] J. B. D. S. L. R. G. West, "Photoacoustic spectroscopy," *Rev. Sci. Instrum.* 54, pp. 797–817, 1983. **10.1063/1.1137483**
- [2] K. W. I. K. V. K. J. Kauppinen, "High sensitivity in gas analysis with photoacoustic detection," *Microchemical Journal*, vol. 76, pp. 151–159, 2004. **10.1016/j.microc.2003.11.007**
- [3] J. K. T. Kuusela, "Photoacoustic gas analysis using interferometric cantilever microphone," *Applied Spectroscopy Reviews*, vol. 42, no. 5, pp. 443–474, 2007. **10.1080/00102200701421755**
- [4] J. P. D. M. M. R. N. S. T. Kuusela, "Photoacoustic gas detection using a cantilever microphone and III–V mid-IR LEDs," *Vibrational Spectroscopy* 51, pp. 289–293, 2009. **10.1016/j.vibspec.2009.08.001**
- [5] M. V. T. H. J. U. S. S. M. M. M. S. L. H. J. Peltola, "High sensitivity trace gas detection by cantilever-enhanced photoacoustic spectroscopy using a mid-infrared continuous-wave optical parametric oscillator," *Opt. Express*, vol. 21, no. 8, pp. 10240–10250, 2013. **10.1364/OE.21.010240**
- [6] M. L. J. Dundurs, "Stress concentration at a sharp edge in contact problems," *Journal of Elasticity*, vol. 2, no. 2, pp. 109–112, 1972. **10.1007/BF00046059**